

Quantitative Analysis of Histone Demethylase Probes Using
Fluorescence PolarizationWenqing Xu,^{†,‡} Jessica D. Podoll,^{†,‡} Xuan Dong,^{†,‡,‡,‡} Anthony Tumber,[§] Udo Oppermann,^{§,||}
and Xiang Wang^{*,†}[†]Department of Chemistry and Biochemistry, University of Colorado, Boulder, Colorado 80309, United States[‡]Department of Developmental Biology, Shandong University, Jinan, Shandong 250100, China[§]Structural Genomics Consortium, University of Oxford, Old Road Campus, Roosevelt Drive, Headington OX3 7DQ, United Kingdom^{||}The Botnar Research Center, NIHR, Oxford Biomedical Research Unit, Oxford OX3 7LD, United Kingdom

S Supporting Information

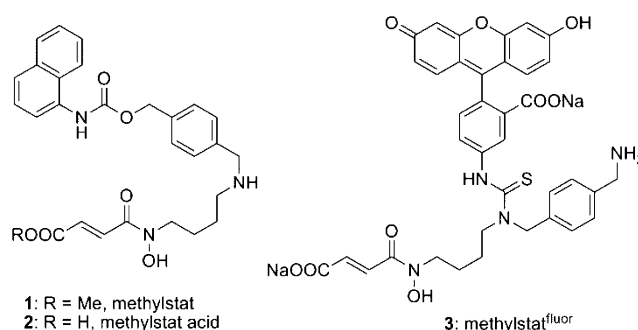
ABSTRACT: We previously reported methylstat as a selective inhibitor of jumonji C domain-containing histone demethylases (JHDMs). Herein, we describe the synthesis of a fluorescent analogue of methylstat and its application as a tracer in fluorescence polarization assays. Using this format, we have evaluated the binding affinities of several known JHDM probes, as well as the native cofactor and substrate of JHDM1A. This fluorophore allowed a highly robust and miniaturized competition assay sufficient for high-throughput screening.

INTRODUCTION

Methylation of histone proteins is one of the most important epigenetic modifications.¹ These reversible modifications recruit effector proteins and trigger a wide range of cellular events, including regulation of gene expression, proliferation, and differentiation. Histone methylations are closely regulated by histone methyltransferases and histone demethylases. Since 2004, two families of enzymes have been reported to exhibit demethylation activities: FAD-dependent monoamine oxidases (LSD1 and 2) and jumonji C domain-containing histone demethylases (JHDMs).² Compared with LSDs, JHDMs have a much broader substrate scope and can modify lysine residues at all methylation states.

Expression of JHDMs plays critical roles in both development and diseases such as cancer and mental retardation.³ Overproduction of 2-hydroxy-glutarate, a natural JHDM inhibitor, due to mutation of isocitrate dehydrogenases, has been identified in multiple cancers.⁴ This development has led to numerous efforts to develop chemical probes targeting JHDMs. Several classes of α -ketoglutarate (α KG) mimics have been developed to inhibit JHDM activity⁵ because all JHDMs use α KG as a cofactor. In addition, a substrate-mimicking small molecule was recently reported to selectively inhibit H3K9-demethylase KIAA1718.⁶ Our group recently discovered a selective, cell-permeable, small-molecule inhibitor methylstat (1, Scheme 1), which was designed as a bivalent substrate-cofactor conjugate.⁷ Its corresponding acid, 2 (Scheme 1), selectively inhibits JHDMs *in vitro*. This bivalent strategy has also proven successful in two very recent reports on JMJD2 class-selective peptidic inhibitors.⁸

Although several classes of JHDM inhibitors have been discovered, determining the selectivity of these inhibitors against various JHDM classes remains a major challenge. This is mainly due to the lack of a uniform biochemical assay for

Scheme 1. Structures of Methylstat (1), Methylstat Acid (2), and Its Fluorescent Analogue Methylstat^{fluor} (3)

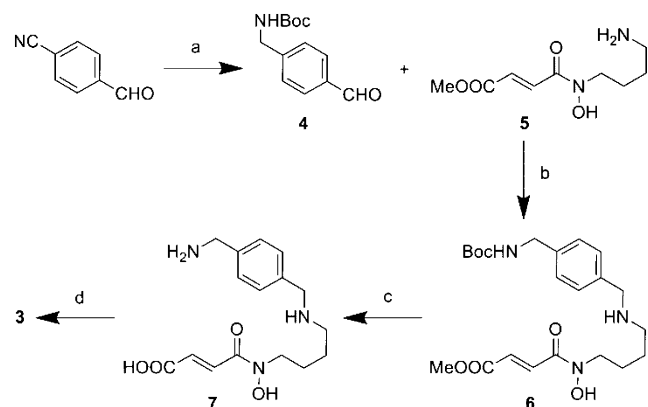
various JHDM isoforms. Most established JHDM biochemical assays are enzyme inhibition assays.^{5a,9} Because of the self-destructive nature of JHDMs under biochemical reaction conditions,¹⁰ these assays typically require optimization for different JHDM isoforms. In addition, they do not allow for accurate measurement of the dissociation constants of the JHDM probes. Thus, the IC₅₀ values derived from these assays cannot be compared directly. Here, we report the synthesis of a fluorescent JHDM probe, 3 (Scheme 1), and the development of a fluorescence polarization (FP)-based binding assay. This assay allows us not only to quantitatively measure the dissociation constants of several JHDM probes but also to validate the inhibitory mechanism of methylstat.

Received: December 17, 2012

RESULTS AND DISCUSSION

The synthesis of fluorophore **3** began with conversion of commercially available 4-cyanobenzaldehyde to aldehyde **4** (Scheme 2),¹¹ which then underwent a reductive amination

Scheme 2. Synthesis of Fluorophore **3**^a



^aReagents and conditions: (a) LiAlH₄, THF, reflux, 12 h, Boc₂O, Et₃N, THF, 25 °C, 12 h, Dess–Martin periodinane, CH₂Cl₂, 25 °C, 30 min, 72% for 3 steps; (b) AcOH, NaBH₃CN, MeOH, 25 °C, 12 h, 59%; (c) TFA, CH₂Cl₂, 0 °C, 30 min, LiOH, THF, H₂O, 25 °C, 2 h, 94% for 2 steps; (d) fluorescein isothiocyanate, satd NaHCO₃/THF, 25 °C, 12 h, 37%.

with amine **5**⁷ to afford secondary amine **6**. The *tert*-butoxycarbonyl (Boc) protecting group of **6** was then removed by trifluoroacetic acid (TFA) and ester hydrolyzed under basic conditions. The resulting diamine (**7**) was treated with fluorescein isothiocyanate (FITC) to afford **3** as the major product.

We next evaluated compound **7** and the fluorescent analogue **3** in the enzyme inhibition assays against JMJD2A and JMJD3, two of the most sensitive JHDMS to methylstat acid (**2**).⁷ Compound **7** showed half-maximum inhibitory concentrations (IC₅₀s) of 2.4 and 7.3 μM against JMJD2A and JMJD3, respectively, which are comparable to those of **2** (i.e., 3.3 and 3.1 μM, respectively). Interestingly, while **3** showed similar activity against JMJD3 with an IC₅₀ of 9.5 μM, it is less active against JMJD2A, with an IC₅₀ of 23.5 μM. Furthermore, the IC₅₀ values of **3** and **7** against JHDM1A were determined as 0.90 and 0.42 μM. These results suggest that selective JHDM

inhibitors may be obtained by modifying the secondary amine of methylstat.

3 shows similar fluorescent properties to fluorescein in pH 7.5 aqueous buffer with the maximum excitation and emission wavelengths as 492 and 517 nm, respectively. With the fluorophore in hand, we set out to develop and optimize an FP binding assay to determine the affinity of fluorophore **3** to various JHDMS. Three JHDMS (JHDM1A, JMJD2A, and JMJD3) from three different classes were evaluated in a saturation binding experiment by following the protocol reported by Rossi and Taylor.¹² FP signals were recorded using the Envision Multilabel plate reader (Perkin-Elmer), and expressed as the change in millipolarization ΔmP, where ΔmP is the mP of the JHDM/**3** mixture minus the mP of **3** only in assay buffer. To determine the dissociation constants (K_d) of **3** and the JHDMS, we plotted JHDM concentrations against ΔmP and fitted the data using eq 1:

$$\Delta mP = [P_{\min} + P_{\max} \times (x/K_d)^n] / [1 + (x/K_d)^n] \quad (1)$$

where, P_{max} and P_{min} are the maximum and minimum observed ΔmP values, respectively, *x* is the JHDM concentration, and *n* is the Hill coefficient of the binding curve. Preliminary tests indicated that **3** bound JHDM1A with the highest affinity among these three JHDMS; therefore, JHDM1A was used for assay optimization.

The initial assay buffer composition was adapted from previous reports on JHDM enzyme activity assays. These generally contain an Fe²⁺ salt and a reducing agent, sodium ascorbate,^{2,7} as Fe²⁺, but not Fe³⁺, is a cofactor for JHDM. Our initial results showed that fluorophore **3** binds to JHDM1A with much higher affinity (K_d: 8.6 ± 1.1 nM) compared with JMJD2A and JMJD3, but the P_{max} was relatively low (<50 mP, Figure 1A). In the absence of any additional metal ions, the P_{max} increased significantly (ca. 120 mP, Figure 1A); however, the K_d of JHDM1A for **3** also increased significantly (19 ± 1.4 nM, Figure 1A). Taken together, these results suggested the loss of the Fe²⁺ during protein purification and protein degradation in the presence of Fe²⁺, a common problem for all Fe²⁺- and αKG-dependent hydroxylases.^{5a} To minimize the effects of Fe²⁺ oxidation, the binding assay was evaluated in the presence of Fe²⁺ under anaerobic conditions; the results were similar to those observed under ambient conditions in the presence of ascorbate.

Because JHDM substrate binding necessitates the addition of metal ions, we next examined the binding in the presence of

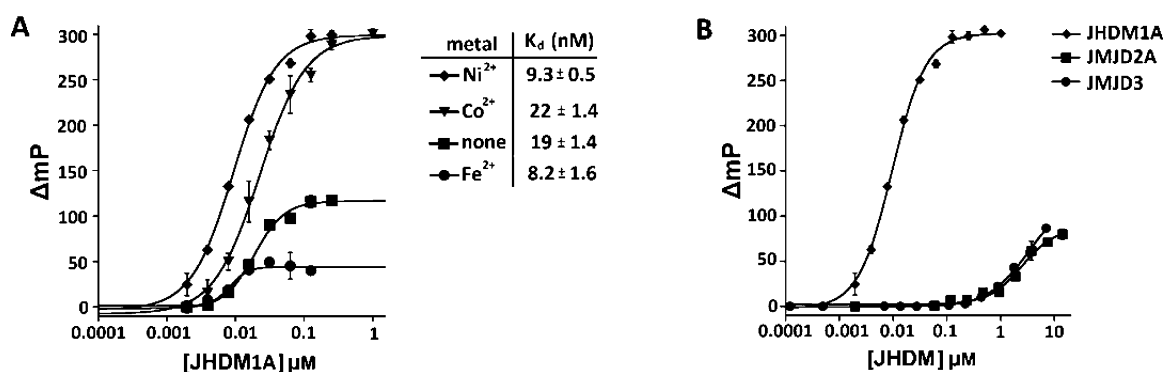


Figure 1. Optimization of the binding conditions for JHDMS and **3**. (A) Binding to JHDM1A was measured with the addition of Fe²⁺, no additional metal, or Ni²⁺ in assay buffer. (B) Binding of **3** to JHDM1A, JMJD2A, and JMJD3 was assessed. Only the binding of JHDM1A and **3** reaches saturation at the concentrations tested.

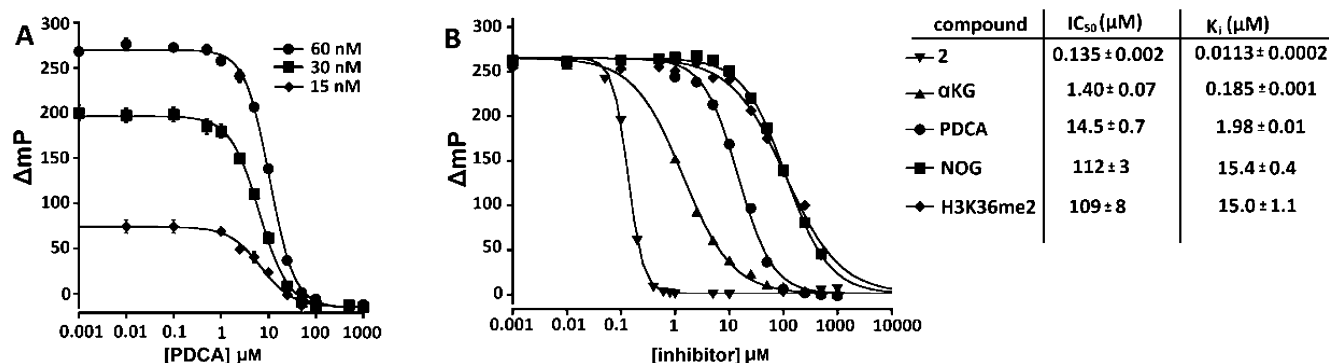


Figure 2. FP competition assay optimization and results. (A) 15, 30, and 60 nM of JHDM1A were tested in the FP competition assay with PDCA. (B) The FP competition assay was used to determine IC₅₀ and K_i values for known JHDM probes.

Ni²⁺ or Co²⁺. Ni²⁺ and Co²⁺ were chosen because they exhibit increased stability under ambient conditions as compared to Fe²⁺. Ni²⁺ and Co²⁺ have been shown to interact with native substrates as well as inhibitors in the JHDM active site in crystallographic studies; furthermore, these transition metals are capable of inhibiting enzyme activation without altering substrate or cofactor binding in the JHDM active site.¹³ Replacement of Fe²⁺ with Ni²⁺ or Co²⁺ in the assay buffer afforded highly stable binding with a much larger dynamic range (ca. 300 mP, Figure 1A). The K_d of JHDM1A for 3 calculated in the presence of Ni²⁺ (9.3 ± 0.5 nM) is more similar to the native condition than that calculated in the presence of Co²⁺ (22 ± 1.4 nM). Hence, we chose to further optimize the FP assay in the presence of Ni²⁺.

We found the binding of JHDM and 3 reached equilibrium after 4 h of incubation at room temperature, and the signals are stable over at least 24 h (Supporting Information (SI) Figure S1). The stabilizing effect of the Ni²⁺ buffer on JHDM1A was also observed by SDS-PAGE analysis (SI Figure S2). JHDM1A in assay buffer containing Fe²⁺ or no additional metal showed significant decomposition after as little as 2 h, whereas JHDM1A in buffer containing Ni²⁺ showed no observable decomposition over the course of 24 h. In addition to the divalent metal ion, we have also optimized the buffer and fluorophore concentration. TRIS buffer provided more consistent results than other buffers such as MOPS and HEPES; a stable and reliable FP signal was achieved using 1 nM fluorophore 3.

Once the assay conditions were optimized for JHDM1A, we reevaluated the binding of 3 with JMJD2A and JMJD3. Although both these enzymes bound 3 at high concentrations, saturation of the FP signal was not achieved at up to 10 μM protein, the highest concentration tested (Figure 1B). Because a protein fluorophore pair with high binding affinity is required for appropriate resolution of nonfluorescent inhibitors in an FP competition assay, further development of the FP competition assay was performed using only JHDM1A.¹⁴

Next, the ability of 3 to serve as a tracer for FP competitive binding experiments was assessed and the appropriate concentration of JHDM1A for FP competition assays optimized. Typically, a protein concentration at which 50–80% of the fluorescent ligand is initially bound is used for FP competition assays but must be optimized to achieve a desirable dynamic range.^{12,14,15} The competition assay was validated and optimized using pyridine 2,4-dicarboxylic acid (PDCA), a well-known αKG mimic, as the competitive ligand (Figure 2A). The competition assay set up was similar to that of the binding assay

except that a constant concentration of protein was used in each condition and the nonfluorescent inhibitor was titrated into the system (5 nM–2 mM). DMSO (1 μL, 1%) was added to each assay well as a vehicle for the inhibitor. Of the three JHDM1A concentrations tested, 60 nM JHDM1A afforded a large dynamic range appropriate for competition assays (Figure 2A); therefore, 60 nM JHDM1A was selected as the protein concentration for the following FP competition studies.

A series of JHDM probes were evaluated in the optimized FP competition assay, such as methylstat acid (2), the JHDM cofactor, αKG, *N*-oxalyl glycine (NOG, an αKG mimic), and the substrate of JHDM1A, an H3K36me2 peptide (Figure 2B).^{5a,13} The results showed that all of the above molecules can displace 3 from JHDM1A. Additionally, the IC₅₀ values stabilized after approximately 4 h and remained stable for up to 24 h. These results not only suggest that 3 binds both the substrate and αKG cofactor-binding sites of JHDM1A but also confirms that methylstat acid (2) is a competitive JHDMs inhibitor.

This competition assay also afforded the half inhibitory concentrations (IC₅₀, Figure 2B) of these JHDM-binding molecules. The IC₅₀ values were then used to calculate their dissociation constants (K_i) with JHDM1A using eq 2 and the online K_i calculator

$$K_i = [I]_{50} / ([L]_{50} / K_d + [P]_0 / K_d + 1) \quad (2)$$

where, [I]₅₀ and [L]₅₀ are free inhibitor concentration and free ligand concentration at 50% inhibition, [P]₀ is free protein concentration at 0% inhibition, and K_d is the dissociation constant between protein JHDM1A and 3.¹⁵

The ability to quantify binding of competitive inhibitors in the JHDM active site is an unprecedented development. Only the binding affinities of some JHDMs relative to histone peptides have been quantified by surface plasmon resonance;^{5a,13c} however, the binding affinity of αKG for various JHDMs has never been reported. Competitive binding assays designed for screening inhibitors have shown relative binding affinities, but report IC₅₀ values of competitive inhibitors as opposed to K_i values. Although IC₅₀ values are useful for assessing the relative effectiveness of inhibitors for a single enzyme, they are not directly comparable between enzymes or between different assays and always depend on the individual assay conditions.¹⁶ Further expansion of our FP binding assay to other JHDM isoforms may be extremely useful for assessing the specificities as well as the inhibitory mechanism of various JHDM probes.

The FP competition assay was further miniaturized to the 384-well plate format. The total volume for each assay was reduced to 20 μL , while the concentrations of JHDM1A (60 nM), fluorophore 3 (1 nM), and DMSO (1%) remained the same. For high-throughput screening purposes, we also evaluated the influence detergent, Tween 20, to our FP assay. We found that addition of 0.1% Tween 20 to the assay buffer completely abolishes the binding, and 0.001% of Tween 20 is well tolerated. To calculate the Z' factor, we used 2 (100 μM in DMSO) and DMSO only as positive and negative controls, respectively. Although the dynamic range of this assay decreased slightly (SI Figure S3), a high Z' factor value (0.78) was calculated,¹⁷ which further demonstrates the robustness of this assay and its suitability for high-throughput screening.

CONCLUSION

We have discovered a fluorescent analogue of methylstat, 3, and have used it to develop an FP binding assay. 3 selectively binds JHDM1A with high affinity (K_d : 9.3 nM) and a large dynamic range (ca. 300 mP). Ni^{2+} ion was found not only to be a good surrogate to the native cofactor Fe^{2+} , but it also stabilizes the protein. The binding of 3 to JHDM1A can be displaced by several known JHDM probes, including its cofactor (αKG), substrate (H3K36me2), and methylstat acid (2). These results confirm that methylstat acid is a bivalent competitive inhibitor of JHDMs. In addition, this FP competition assay allows quantitative measurement of K_i values of nonfluorescent JHDM1A active site binding molecules. It is also noteworthy that the K_i of αKG and JHDM1A was determined, which has previously been impossible and illustrates the utility of our FP binding assay for quantifying the binding affinities of native JHDM substrates quickly and easily. Furthermore, we were able to use our FP system to develop a highly robust and miniaturized assay appropriate for high-throughput screening of large compound libraries (Z' : 0.78). Further optimization of the fluorophore for the development of FP assays appropriate for other JHDMs is ongoing and will be reported in due course.

EXPERIMENTAL SECTION

Synthetic procedure for the preparation of fluorophore 3, characterization data, and NMR spectra of all new compounds are in SI.

Protein Expression and Purification. Recombinant JHDM1A (1–517) and JMJD3 (1018–1590) were expressed as 6XHis fusion proteins using the pNIC28 and the pNH-TrxT expression vectors, respectively. The coding regions were verified by sequencing and the plasmids were transfected into BL21 *Escherichia coli*. Following expression, JHDM1A was purified using Ni SepharoseTM 6 Fast Flow beads (GE) by gravity chromatography according to the manufacturer's instructions. JMJD3 was purified using cobalt (high density) agarose beads (Gold Biotechnology) according to the manufacturer's protocol. JMJD2A was expressed and purified as described previously.⁷ The purified proteins were exchanged into assay buffer, flash frozen in liquid nitrogen, and stored at -80°C .

FP Binding Assay. FP binding experiments were performed in black, low-binding, half area 96-well plates (Corning 3993). Then 80 μL of JHDM1A (2.44 nM to 2.50 μM in 2-fold dilution) in assay buffer (50 μM NiCl_2 , 25 mM TRIS, 100 mM NaCl, pH 7.5) were added to experimental wells. After 10 min, 20 μL of 3 (5 nM in assay buffer) was then added to each well. Wells containing protein only were subtracted from assay wells as background. Plates were incubated at room temperature and read five times at each time point (1, 2, 4, 6, 8, 10, and 24 h), and the average values at each time point were used for the calculation of the polarization values. Binding curves were fit using KaleidaGraph (v4.1.1, Synergy Software).

FP Competitive Binding Assay. Known JHDM active site binders (2, αKG , PDCA, NOG, or peptide H3K36me2) were tested for their ability to compete the binding of 3 to JHDM1A. Then 2-fold serial dilutions of compounds were prepared as 100 \times solutions in DMSO. Then 80 μL of JHDM1A (75 nM in assay buffer) were added to each well, to which 1 μL of the above compound solutions were added. The mixtures were incubated at room temperature for 30 min prior to addition of 20 μL of 3 (5 nM in assay buffer). Controls containing 3 and JHDM1A or JHDM1A and the competing compound were included for background subtraction. Each experiment was performed in duplicate. The assay plates were incubated at room temperature for 4 h before signals were recorded by the Envision Multilabel plate reader. The calculated data was fitted using KaleidaGraph (v4.1.1, Synergy Software).

ASSOCIATED CONTENT

Supporting Information

Experimental details for the syntheses and spectroscopic characterization of the compounds, as well as determination of Z' factor experiment and result in this paper. This material is available free of charge via the Internet at <http://pubs.acs.org>.

AUTHOR INFORMATION

Corresponding Author

*Phone (303) 492-6266. E-mail: xiang.wang@colorado.edu.

Author Contributions

[†]These authors contributed equally.

Notes

The authors declare no competing financial interest.

ACKNOWLEDGMENTS

This work was supported by the University of Colorado Boulder, and by the National Institutes of Health under grant no. R01-GM098390, and the institutional training grant GM008732 to J.D.P. X.D. thanks the China Scholarship Council for a Visiting Student Scholarship. The Structural Genomics Consortium is a registered charity (no. 1097737) that receives funds from Abbvie, Boehringer Ingelheim, the Canadian Institutes for Health Research, the Canadian Foundation for Innovation, Eli Lilly and Company, Genome Canada, GlaxoSmithKline, the Ontario Ministry of Economic Development and Innovation, Janssen, the Novartis Research Foundation, Pfizer, Takeda, and the Wellcome Trust. U.O. is also supported by BBSRC, Bayer Healthcare and Oxford NIHR Biomedical Research Unit.

ABBREVIATIONS USED

JHDM, jumonji C domain-containing histone demethylase; αKG , α -ketoglutarate; FP, fluorescence polarization; Boc, *tert*-butoxycarbonyl; TFA, trifluoroacetic acid; FITC, fluorescein isothiocyanate; PDCA, pyridine 2,4-dicarboxylic acid; NOG, *N*-oxalyl glycine; K_d , dissociation constant; IC_{50} , half-maximum inhibitory concentration; K_i , dissociation constant of inhibitor

REFERENCES

- (1) Greer, E. L.; Shi, Y. Histone methylation: a dynamic mark in health, disease and inheritance. *Nature Rev. Genet.* **2012**, *13*, 343–357.
- (2) Shi, Y.; Whetstone, J. R. Dynamic regulation of histone lysine methylation by demethylases. *Mol. Cell* **2007**, *25*, 1–14.
- (3) Pedersen, M. T.; Helin, K. Histone demethylases in development and disease. *Trends Cell Biol.* **2010**, *20*, 662–671.
- (4) Chowdhury, R.; Yeoh, K. K.; Tian, Y. M.; Hillringhaus, L.; Bagg, E. A.; Rose, N. R.; Leung, I. K.; Li, X. S.; Woon, E. C.; Yang, M.; McDonough, M. A.; King, O. N.; Clifton, I. J.; Klose, R. J.; Claridge, T.

D.; Ratcliffe, P. J.; Schofield, C. J.; Kawamura, A. The oncometabolite 2-hydroxyglutarate inhibits histone lysine demethylases. *EMBO Rep.* **2011**, *12*, 463–469.

(5) (a) Rose, N. R.; McDonough, M. A.; King, O. N.; Kawamura, A.; Schofield, D. J. Inhibition of 2-oxoglutarate dependent oxygenases. *Chem. Soc. Rev.* **2011**, *40*, 4364–4397. and references therein.

(b) Kruidenier, L.; Chung, C. W.; Cheng, Z.; Liddle, J.; Che, K.; Joberty, G.; Bantscheff, M.; Bountra, C.; Bridges, A.; Diallo, H.; Eberhard, D.; Hutchinson, S.; Jones, E.; Katso, R.; Leveridge, M.; Mander, P. K.; Mosley, J.; Ramirez-Molina, C.; Rowland, P.; Schofield, C. J.; Sheppard, R. J.; Smith, J. E.; Swales, C.; Tanner, R.; Thomas, P.; Tumber, A.; Drewes, G.; Oppermann, U.; Patel, D. J.; Lee, K.; Wilson, D. M. A selective jumonji H3K27 demethylase inhibitor modulates the proinflammatory macrophage response. *Nature* **2012**, *488*, 404–408.

(6) Upadhyay, A. K.; Rotili, D.; Han, J. W.; Hu, R.; Chang, Y.; Labella, D.; Zhang, X.; Yoon, Y. S.; Mai, A.; Cheng, X. An analog of BIX-01294 selectively inhibits a family of histone H3 lysine 9 Jumonji demethylases. *J. Mol. Biol.* **2012**, *416*, 319–327.

(7) Luo, X.; Liu, Y.; Kubicek, S.; Myllyharju, J.; Tumber, A.; Ng, S.; Che, K. H.; Podoll, J.; Heightman, T. D.; Oppermann, U.; Schreiber, S. L.; Wang, X. A selective inhibitor and probe of the cellular functions of Jumonji C domain-containing histone demethylases. *J. Am. Chem. Soc.* **2011**, *133*, 9451–9456.

(8) (a) Lohse, B.; Nielsen, A. L.; Kristensen, J. B. L.; Helgstrand, C.; Cloos, P. A.; Olsen, L.; Gajhede, M.; Clausen, R. P.; Kristensen, J. L. Targeting histone lysine demethylases by truncating the histone 3 tail to obtain selective substrate-based inhibitors. *Angew. Chem., Int. Ed.* **2011**, *50*, 9100–9103. (b) Woon, E. C. Y.; Tumber, A.; Kawamura, A.; Hillringhaus, L.; Ge, W.; Rose, N. R.; Ma, J. H. Y.; Chan, M. C.; Walport, L. J.; Che, K. H.; Ng, S. S.; Marsden, B. D.; Oppermann, U.; McDonough, M. A.; Schofield, C. J. Linking of 2-oxoglutarate and substrate binding sites enables potent and highly selective inhibition of JmjC histone demethylases. *Angew. Chem., Int. Ed.* **2012**, *51*, 1631–1634.

(9) Krishnan, S.; Collazo, E.; Ortiz-Tello, P. A.; Trievel, R. C. Purification and assay protocols for obtaining highly active Jumonji C demethylases. *Anal. Biochem.* **2012**, *420*, 48–53.

(10) Mantri, M.; Zhang, Z.; McDonough, M. A.; Schofield, C. J. Autocatalysed oxidative modifications to 2-oxoglutarate dependent oxygenases. *FEBS J.* **2012**, *279*, 1563–1575.

(11) Far, A. R.; Cho, Y. L.; Rang, A.; Rudkevich, D. M.; Rebek, J. Polymer-bound self-folding cavitands. *Tetrahedron* **2002**, *58*, 741–755.

(12) Rossi, A. M.; Taylor, C. W. Analysis of protein–ligand interactions by fluorescence polarization. *Nature Protoc.* **2011**, *6*, 365–387.

(13) (a) Couture, J. F.; Collazo, E.; Ortiz-Tello, P. A.; Brunzelle, J. S.; Trievel, R. C. Specificity and mechanism of JMJD2A, a trimethyllysine-specific histone demethylase. *Nature Struct. Mol. Biol.* **2007**, *14*, 689–195. (b) Ng, S. S.; Kavanagh, K. L.; McDonough, M. A.; Butler, D.; Pilka, E. S.; Lienard, B. M.; Bray, J. E.; Savitsky, P.; Gileadi, O.; von Delft, F.; Rose, N. R.; Offer, J.; Scheinost, J. C.; Borowski, T.; Sundstrom, M.; Schofield, C. J.; Oppermann, U. Crystal structures of histone demethylase JMJD2A reveal basis for substrate specificity. *Nature* **2007**, *448*, 87–91. (c) Horton, J. R.; Upadhyay, A. K.; Qi, H. H.; Zhang, Z.; Shi, Y.; Cheng, X. Enzymatic and structural insights for substrate specificity of a family of jumonji histone lysine demethylases. *Nature Struct. Mol. Biol.* **2010**, *17*, 38–43. (d) Sekirnik, R.; Rose, R. R.; Mecinović, J.; Schofield, C. J. 2-Oxoglutarate oxygenases are inhibited by a range of transition metals. *Metallomics* **2010**, *2*, 397–399.

(e) Sengoku, T.; Yokoyama, S. Structural basis for histone H3 Lys 27 demethylation by UTX/KDM6A. *Genes Dev.* **2011**, *25*, 2266–2277.

(14) Huang, X. Fluorescence polarization competition assay: the range of resolvable inhibitor potency is limited by the affinity of the fluorescent ligand. *J. Biomol.* **2003**, *8*, 34–38.

(15) (a) Nikolovska-Coleska, Z.; Wang, R.; Fang, X.; Pan, H.; Tomita, Y.; Li, P.; Roller, P. P.; Krajewski, K.; Saito, N. G.; Stuckey, J. A.; Wang, S. Development and optimization of a binding assay for the XIAP BIR3 domain using fluorescence polarization. *Anal. Biochem.* **2004**, *332*, 261–273. (b) *The Ki Calculator for Fluorescence-Based*

Competitive Binding Assays; University of Michigan: Ann Arbor, MI, 2004; sw16.im.med.umich.edu/software/calc_ki.

(16) Krohn, K. A.; Link, J. M. Interpreting enzyme and receptor kinetics: keeping it simple, but not too simple. *Nuclear Med. Biol.* **2003**, *30*, 819–826.

(17) Zhang, J. H.; Chung, T. D.; Oldenburg, K. R. A simple statistical parameter for use in evaluation and validation of high throughput screening assays. *J. Biomol. Screening* **1999**, *4*, 67–73.